

Computation of 2-D Spectra Assisted by Compressed Sampling

J. Almeida^{1,2}, J. Prior³ and M.B. Plenio^{1,2}

¹ *Institute for Theoretical Physics, Albert-Einstein-Allee 11, University Ulm, D-89069 Ulm, Germany*

² *Institute for Integrated Quantum Science and Technology,*

Albert-Einstein-Allee 11, University Ulm, D-89069 Ulm, Germany and

³ *Departamento de Física Aplicada, Universidad Politecnica de Cartagena, Cartagena 30202, Spain*

The computation of scientific data can be very time consuming even if they are ultimately determined by a small number of parameters. The principle of compressed sampling suggests that for typical data we can achieve a considerable decrease in the computation time by avoiding the need to sample the full data set. We demonstrate the usefulness of this approach at the hand of 2-D spectra in the context of ultra-fast non-linear spectroscopy of biological systems where numerical calculations are highly challenging due to the considerable computational effort involved in obtaining individual data points.

Introduction – Signals of interest that are obtained in experiments or by numerical computation of natural phenomena are not white noise but contain hidden structure and redundancy. The fact that it is possible to make use of these structures is the basis of compressed sampling [1–4] which demonstrates, surprisingly, that the accurate reconstruction of such signals can be achieved with high probability from a number of data points that would be deemed insufficient by the Nyquist - Shannon criterion. This promise of considerable efficiency gains together with the development of numerical algorithms that allow for its efficient implementation have led to an explosion of applications of compressed sampling in signal processing [5].

Here we apply the principle of compressed sampling to the problem of non-linear two-dimensional (2-D) spectroscopy and demonstrate that its application can offer a considerable reduction in the computational effort involved in the numerical determination of such spectra. This makes accessible 2-D spectra for larger systems or for systems that are governed by more complex dynamical equations, for example due to the inclusion of non-Markovian features [6–9]. This computational saving is not restricted to 2-D spectra. It serves however to highlight the observation that numerical computation of signals arising in nature can be made considerably more efficient employing the paradigm of compressed sampling. This is true whenever the signal is determined by a small number of parameters but the computation of individual data points is very costly [10, 11]. It is noteworthy that the same ideas may also be applied to reduce the experimental effort in measuring 2-D spectra. Here however the impact of experimental noise on the quality of this reconstruction requires careful consideration [12] and will be studied elsewhere.

Principles – In non-linear 2-D spectroscopy a series of three (or more) laser pulses is used to probe the dynamics of a system and the resulting information is arranged as a matrix representing the two dimensional Fourier transform of the signal which in turn describes the system response in dependence of the spacing between laser pulses

(more details will be given in the next section). The point by point computation of the entries of this matrix can be very time consuming, especially when the relevant dynamical system is high-dimensional or subject to a complex non-Markovian system-environment interaction. As explained above, we expect however that this matrix contains structure. In line then with the paradigm of compressed sampling it will be possible to achieve a considerable reduction in the number of elements of the signal that need to be obtained through (random) sampling (by experimental observation or numerical computation). After an outline of the numerical algorithm that is being used we provide a demonstration of the achievable computational gain at the hand of a specific biomolecular complex of current interest.

Let M be an $n \times n$ matrix that represents the 2-D spectrum that we wish to reconstruct and let experimental observation or numerical computation determine a small subset of these elements described by the set of indices Ω . Denoting by $tr|X|$ the trace norm of a matrix X it can be proven that the solution of the minimization problem

$$\min[tr|X| : X_{ij} = M_{ij} \text{ for } (i, j) \in \Omega] \quad (1)$$

is *unique* and yields the matrix M with a probability larger than $1 - \exp(-\beta)$ if the number of sampled entries of M is of order $nr(1 + \beta) \ln n$, where $\beta > 0$ is an arbitrary constant and r is the rank of the matrix M (see [13, 14] for proofs and a rigorous mathematical statement). While reconstruction of the matrix M cannot be guaranteed with certainty, the probability for obtaining the correct reconstruction of the matrix M can be increased arbitrarily by repeating the sampling and reconstruction procedure k times. Accepting the majority result increases the probability that the so obtained result is correct to above $1 - e^{-k\beta}$. For typical values of n in the range of 100 – 1000 only $\beta = \ln n$ this reduces the probability of a wrong reconstruction to $10^{-8} - 10^{-12}$. Given that the computation time for the full data set scales as n^2 this suggest that a considerable potential reduction in computational effort is possible.

The solution of the minimization problem eq. (1) can

be obtained by standard solvers for semidefinite optimization problems which do however tend to be limited to relatively small matrix sizes with several hundred elements only. Here we solve the minimization problem of eq. (1) by means of the so-called singular value thresholding (SVT) algorithm [15, 16] which permits very large matrices to be treated and to provably approximate the solution of eq. (1) to arbitrary precision. The SVT-algorithm solves iteratively the set of equations

$$Y^{(k-1)} = U^{(k-1)} D^{(k-1)} V^{(k-1)} \quad (2)$$

$$X^{(k)} = U^{(k-1)} \max(D^{(k-1)} - \tau \mathbb{1}, 0) V^{(k-1)} \quad (3)$$

$$Y^{(k)} = Y^{(k-1)} + \delta \mathcal{P}_\Omega(M - X^{(k)}) \quad (4)$$

where $\mathcal{P}_\Omega(M)$ is a matrix whose entries satisfy $(\mathcal{P}_\Omega(M))_{ij} = M_{ij}$ for $(i, j) \in \Omega$ and are zero otherwise while τ and δ are constants whose choice will be described below. The algorithm is initialized by a random matrix $Y^{(0)}$ for the first iteration $k = 1$. Then the singular value decomposition of $Y^{(0)}$ is computed in eq. (2). This is followed by the so-called soft thresholding step eq. (3) where we subtract from all the singular values the parameter τ and set negative results to 0. This step yields a matrix $X^{(k)}$ that has lower rank than $Y^{(k-1)}$. The final step of iteration k then uses $X^{(k)}$ to construct a matrix $Y^{(k)}$ that satisfies the constraints $X_{ij} = M_{ij}$ for $(i, j) \in \Omega$ more closely than the matrix $Y^{(k-1)}$ eq. (4). These steps are iterated until convergence has been achieved.

The choice $\delta < 2$ ensure provable convergence of the iteration. For τ the choice $\tau = 5n$ for $n \times n$ -matrices leads to fast convergence and very close approximation to the solution of eq. (1) (see [15] for details). Making use of the sparseness of the matrices the SVT algorithm is capable of treating very large matrices (reaching 30000×30000 and above). Variants of this algorithm can achieve a considerable additional increase in computational efficiency [17, 18] by employing linear time algorithms for the implementation of the singular value decomposition in eq. (2).

Whenever the calculation of individual data points is costly, it will be advantageous to apply the compressed sampling paradigm and compute only a small subset of the matrix elements and complete the remaining entries of the matrix with the SVT algorithm. In the following we would like to demonstrate the power of this approach in the calculation of 2-D spectra.

Applications – Non-linear spectroscopy has proven to be useful in order to unveil the dynamics involved in excitonic transfer of light harvesting complexes, due to the fact that it is sensitive to excitonic quantum superpositions, i.e., excitonic coherences [20–23] as well as vibrational features of the protein environment [24, 25]. Non-linear 2-D spectroscopy can resolve the third-order polarization of the electronic system, from the signal $S^{(3)}(t_1, t_2, t_3)$, arising from photo-excitation of three consecutive pulses with wave vectors \mathbf{k}_1 , \mathbf{k}_2 and \mathbf{k}_3 , sepa-

rated by time intervals t_1 and t_2 and measured at a time t_3 after the last pulse. It is customary to Fourier transform the time t_1 and t_3 dimensions to yield $S(\omega_1, t_2, \omega_3)$ in order to generate a 2-D spectra parametrized by the waiting time t_2 . The numerical computation as well as the experimental determination of these 2-D spectra represent a challenging task because of the large number of measurements that need to be taken and the considerable computational resources required for the determination of $S^{(3)}(t_1, t_2, t_3)$.

Here we will demonstrate by means of numerical examples, that the paradigm of compressed sampling delivers a considerable gain in computational efficiency as it is not necessary to determine the full signal $S^{(3)}(t_1, t_2, t_3)$ for a given choice of t_2 . The computation for a randomly chosen subset of times t_1, t_3 suffice to reconstruct the full signal.

We consider the 2-D spectra of a pigment-protein complex, the Fenna-Matthews-Olson (FMO) complex, which has received considerable attention recently [23]. In a spectroscopy experiment the pigment-protein complex dynamics is probed by means of applying different laser pulses and measuring the response to them. Using Liouville space notation we can describe the evolution of our system under the effect of the laser pulses by the master equation

$$\frac{d\rho}{dt} = -\frac{i}{\hbar} \mathcal{L} \rho - \frac{i}{\hbar} \mathcal{L}_{\text{int}}(t) \rho. \quad (5)$$

Here the Liouvillian \mathcal{L} describes the internal excitation dynamics including dephasing of the complex while the term $\mathcal{L}_{\text{int}}(t)$ stands for the interaction with the laser. Typically in these complexes the dissipation time scales are much longer than the dephasing induced by the environment and hence we will consider only pure dephasing contributions to the internal dynamics. That is, we will consider an unperturbed Liouvillian with the form $\mathcal{L} \equiv \mathcal{L}_{\text{Ham}} + \mathcal{L}_{\text{deph}}$. Within the Born-Markov approximation we can write each of the terms in the equations above as:

$$\mathcal{L}_{\text{Ham}} \equiv [H_s, \rho] \quad (6)$$

$$\mathcal{L}_{\text{deph}} \equiv i \sum_{i=1}^7 2\gamma_i (\sigma_i^z \rho \sigma_i^z - \rho) \quad (7)$$

$$\mathcal{L}_{\text{int}}(t) = [H_{\text{int}}(t), \rho], \quad (8)$$

with σ_x , σ_y , σ_z the standard Pauli matrices and $H_{\text{int}} = -\vec{E}(t) \cdot \vec{V}$. For the homogeneous dephasing rates we have chosen random values within a realistic interval for each chromophore, i.e., $\{\gamma_i\}_{i=1..7} = \{0.94, 2.26, 2.83, 1.70, 1.70, 1.88, 2.07\} \times 10^{-3} \text{rad/fs}$ (with the conversion $1 \text{rad} \cdot \text{fs}^{-1} / 1 \text{cm}^{-1} = 2\pi \cdot 2.99792458 \times 10^{-5}$), which correspond to dephasing times in the scale of few picoseconds. As regards the actual values of

the site energies and intersite coupling rates in the one-

exciton sector we have used the following Hamiltonian[27] (in units of rad/fs):

$$H_s = \begin{pmatrix} 0.0405 & -0.0224 & 0.0013 & -0.0014 & 0.0016 & -0.0034 & -0.0028 \\ -0.0224 & 0.0575 & 0.0070 & 0.0018 & 0.0004 & 0.0031 & 0.0013 \\ 0.0013 & 0.0070 & 0 & -0.0131 & -0.0003 & -0.0022 & 0.0007 \\ -0.0014 & 0.0018 & -0.0131 & 0.0377 & -0.0147 & -0.0040 & -0.0143 \\ 0.0016 & 0.0004 & -0.0003 & -0.0147 & 0.0801 & 0.0208 & -0.0012 \\ -0.0034 & 0.0031 & -0.0022 & -0.0040 & 0.0208 & 0.0593 & 0.0081 \\ -0.0028 & 0.0013 & 0.0007 & -0.0143 & -0.0012 & 0.0081 & 0.0499 \end{pmatrix} + 2.297 \cdot \mathbf{1}. \quad (9)$$

Finally, the dipolar operator is defined from the individual dipole momenta of each chromophore $\{\vec{\mu}_i\}_{i=1\dots 7}$ as $\vec{V} = \sum_{i=1}^7 \vec{\mu}_i \sigma_i^x$. The directions of the seven induced-transition dipoles $\vec{\mu}_i$, extracted from the structure of the FMO complex [28], are

$$\frac{[\mu_i]}{|\vec{\mu}_{\text{BCh}}|} = \begin{pmatrix} -0.026 & 0.286 & -0.958 \\ -0.752 & 0.601 & -0.271 \\ -0.935 & 0.061 & 0.349 \\ -0.001 & 0.393 & -0.919 \\ -0.739 & 0.672 & 0.048 \\ -0.859 & 0.371 & -0.353 \\ -0.176 & -0.042 & -0.983 \end{pmatrix} \quad (10)$$

and their magnitude is taken to be the same and given in units of the dipole strength $|\vec{\mu}_{\text{BCh}}|$ of an isolated bacteriochlorophyll.

The signal measured on a general spectroscopic experiment is intimately related to the system electric response functions of different orders $S^{(n)}$. In particular in non-linear 2-D spectroscopy experiments the signal can be related to the third-order response function $S^{(3)}(t_1, t_2, t_3)$. This function can be written in a very compact form using tetradic notation in Liouville space [20]

$$S^{(3)}(t_1, t_2, t_3) = \left(\frac{i}{\hbar}\right)^3 \langle\langle V | \mathcal{G}(t_3) \mathcal{V} \mathcal{G}(t_2) \mathcal{V} \mathcal{G}(t_1) \mathcal{V} | \rho(-\infty) \rangle\rangle \quad (11)$$

where $\mathcal{G}(t)$ is the Liouville space Green Function in the absence of the radiation field

$$\mathcal{G}(t) \equiv \theta(t) \exp\left(\frac{i}{\hbar} \mathcal{L}t\right) \quad (12)$$

and the action of the superoperator \mathcal{V} upon an ordinary operator A is defined as

$$\mathcal{V}A \equiv [V, A]. \quad (13)$$

The dynamics of a photo-reactive molecule interacting with a series of laser beams does not preserve the number of excitations within the molecule. If we consider the natural assumption that the system is in its

ground state when the first pulse arrives at the sample (i.e., $\rho(-\infty) = |g\rangle\langle g|$), then the only relevant sectors to compute the third-order response function are the ground state itself, the one-exciton and the two-excitons manifolds. In FMO, with seven chromophores, this accounts for $1 + 7 + 21 = 29$ states, which means that any operator in Hilbert space can be represented as a matrix of dimensions 29×29 , while a superoperator acting on the Liouville space can be represented by matrices of dimension $29^2 \times 29^2$. On the other hand, the only operators needed to compute the response function from eq. (11) are the total Hamiltonian of the FMO molecule (and the corresponding Liouvillian \mathcal{L}_{Ham}), the dephasing superoperator $\mathcal{L}_{\text{deph}}$ and the total dipolar operator V (with the corresponding superoperator \mathcal{V}). It is indeed a straightforward procedure to construct these operators in the manifolds mentioned above [26] and it should be noted that the only information required to construct them are the physical matrix elements given by H_s in eq. (9), together with the dipole information contained in eq. (10) and the dephasing rates $\{\gamma_i\}_{i=1\dots 7}$ already written above.

Results of the application of compressive sampling on these 2-D spectra are presented in Fig. 1 for population time $t_2 = 0$. Already computing only about 0.16% randomly sampled points (topleft) the position of peaks start to emerge. For higher sampling ratios of 1% (bottomleft) many features of the spectrum are reproduced qualitatively even though some minor features are missing. For 8% (topright) the spectra are reproduced very well quantitatively and the differences with the exact 2-D spectra (bottomright) are almost negligible as quantified by the Frobenius norm difference (see caption of Fig. 1). Note that all the spectra have been normalized to the same maximum value for ease of comparison. The reconstruction of the 600×600 -matrices from the randomly sampled points was possible within less than 1 minute on a standard laptop for $S^{(3)}(t_1, t_2 = 0, t_3)$ [29]. The full computation of such a spectrum on the same machine takes around 60 minutes and scales as n^2 for an $n \times n$ matrix. Assuming a sampling of 1% of the data set the same calculation could have been achieved in around 2

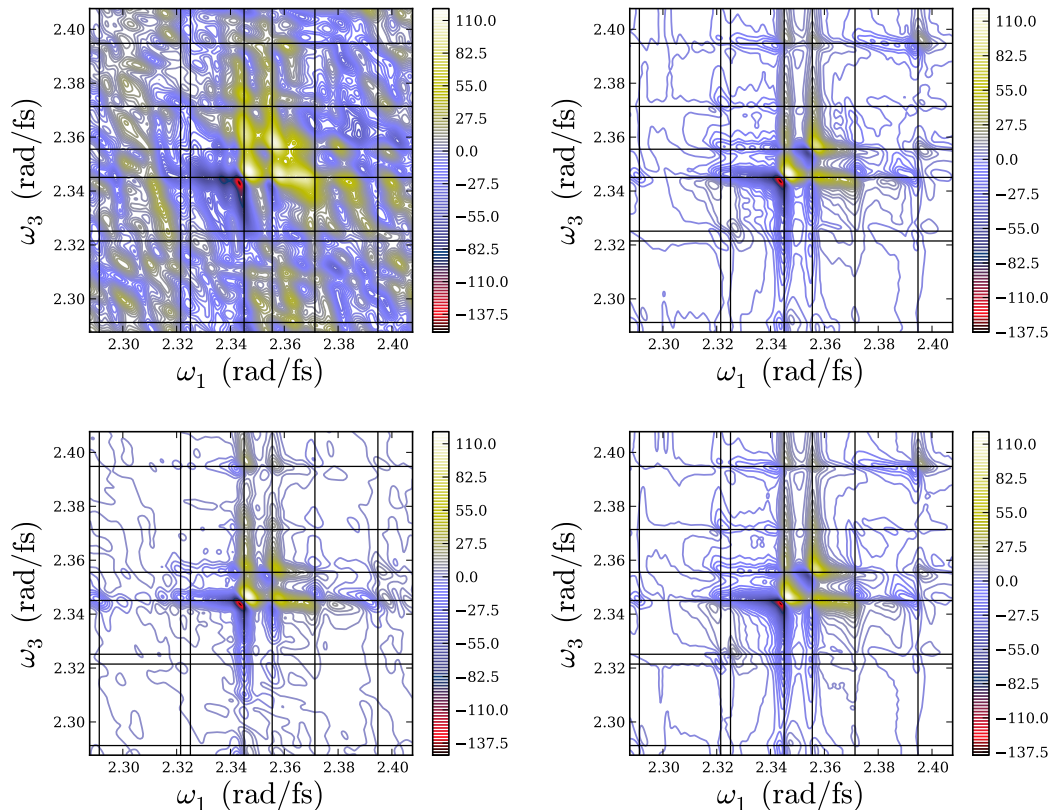


FIG. 1. The 2-D spectrum of the FMO complex with $t_2 = 0$ (with the parameters described in the text) for a random sampling of (topleft) 0.16%, (bottomleft) 1%, (topright) 8% of the total data set $S^{(3)}(t_1, t_2 = 0, t_3)$ and the exact spectrum (bottomright). The black lines indicate the eigenfrequencies of the Hamiltonian in the first exciton manifold. Even for very small sampling rates the principal features of the spectrum are well reproduced and for a sampling of 8% only very minor differences remain. Each time variable has 600 bins resulting in a total data set in the form of a 600×600 matrix. The convergence of the reconstructed matrices S_k to the exact spectrum S_{ex} with increasing sampling k can also be quantified using the standard Frobenius norm with the magnitude $\mathcal{D}_k \equiv \|S_{\text{ex}} - S_k\| / \|S_{\text{ex}}\|$ which yields $\{\mathcal{D}_k\}_{k=0.16, 1.00, 8.00} = \{1.81, 0.38, 0.08\}$. For the sake of comparison, the same measure averaged over a large sample of entirely random matrices S_{rand} yields $\mathcal{D}_{\text{rand}} = 8.96$. On the other hand, the most distant matrix from the exact spectrum gives $\mathcal{D}_{\text{worst}} = 15.72$.

minutes including the SVT reconstruction implying a 30 fold improvement in computation time. The relative efficiency improvement grows almost linearly with n . It should also be noted that 2-D spectra simulations aimed at direct comparison with experiments typically include rotational and inhomogeneous averages that would multiply the total computation time by the size of the sampling distribution used to make each independent averaging. This does not affect our general conclusion concerning the computational speedup that can be obtained by means of compressive sampling.

This example shows that even for rich 2-D spectra such as those obtained for the FMO complex, compressive sampling yields a considerable reduction of the number of arguments t_1, t_3 for the which $S^{(3)}(t_1, t_2 = 0, t_3)$ needs to be evaluated to obtain the complete 2-D spectrum with a precision that is sufficient for comparison to experiment. This exemplifies the power of signal processing concepts to save computational resources. The extraction of in-

formation from complex spectra can also be assisted by methods from signal processing and in a future publication we will explore the use of wavelets to this effect.

Conclusions – We have demonstrated that the principles of compressed sampling can lead to significant reductions in the computation of non-linear 2-D spectra. In such cases only a small number of data points need to be determined while the rest is constructed via matrix reconstruction techniques. Our findings are more general however and can provide considerable computational savings in a wide variety of computational problems in physics where data are represented by low-rank matrices.

Acknowledgements – We acknowledge discussions with T. Baumgratz, F. Caycedo-Soler, M. Cramer and S.F. Huelga. This work was supported by an Alexander von Humboldt Professorship, the EU Integrated Project QESSENCE, the BMBF Verbundprojekt QuORP, the Ministerio de Ciencia e Innovación Project No. FIS2009-13483-C02-02 and the Fundación Séneca Project No.

-
- [1] E.J. Candes and M.B. Wakin, An introduction to compressive Sampling, *IEEE Signal Processing Magazine* **25** **2008**, 21-30
- [2] E. Candes, J. Romberg and T. Tao, Robust uncertainty principles: Exact signal reconstruction from highly incomplete frequency information, *IEEE Trans. Inform. Theory*. **2006**, 52, 489 - 509.
- [3] E. Candes and T. Tao, Near optimal signal recovery from random projections: Universal encoding strategies, *IEEE Trans. Inform. Theory*. **2006**, 52, 5406 - 5425.
- [4] D. Donoho, Compressed Sensing, *IEEE Trans. Inform. Theory*. **2006**, 52, 1289 - 1306.
- [5] See <http://dsp.rice.edu/cs> for a selection of review articles on compressive sensing.
- [6] A. Ishizaki and G.R. Fleming, Unified treatment of quantum coherent and incoherent hopping dynamics in electronic energy transfer: Reduced hierarchy equation approach, *J. Chem. Phys.* **2009**, 130, 234111 (10 pages).
- [7] J. Prior, A.W. Chin, S.F. Huelga and M.B. Plenio, Efficient simulation of strong system-environment interactions, *Phys. Rev. Lett.* **2010**, 105, 050404 (4 pages).
- [8] A.W. Chin, A. Rivas, S.F. Huelga and M.B. Plenio, Exact mapping between system-reservoir quantum models and semi-infinite discrete chains using orthogonal polynomials, *J. Math. Phys.* **2010**, 51, 092109 (20 pages).
- [9] Ch. Kreisbeck and T. Kramer, Long-Lived Electronic Coherence in Dissipative Exciton-Dynamics of Light-Harvesting Complexes, *E-print arXiv:1203.1485* **2012** (7 pages).
- [10] X. Andrade, J. N. Sanders, A. Aspuru-Guzik, Application of compressed sensing to the simulation of atomic systems, *E-print arXiv:1205.6485* **2012** (7 pages).
- [11] J. N. Sanders, S. Mostame, S. K. Saikin, X. Andrade, J. R. Widom, A. H. Marcus, A. Aspuru-Guzik, Compressed sensing for multidimensional electronic spectroscopy experiments, *E-print arXiv:1207.3766* **2012** (5 pages).
- [12] E.J. Candes and Y. Plan, Matrix completion with noise, *Proc. IEEE* **2010**, 98, 925 - 936.
- [13] E. Candes and B. Recht, Exact Matrix Completion via Convex Optimization, *Found. Comp. Math.* **2009**, 9, 717 - 772.
- [14] D. Gross, Recovering Low-Rank Matrices From Few Coefficients In Any Basis, *IEEE Trans. Inf. Theo.* **2011**, 57, 1548 - 1566.
- [15] J.-F. Cai, E.J. Candes and Z. Shen, A singular value thresholding algorithm for matrix completion, *SIAM J. Opt.* **2010**, 20, 1956 - 1982.
- [16] M. Cramer, M.B. Plenio, S.T. Flammia, R. Somma, D. Gross, S.D. Bartlett, O. Landon-Cardinal, D. Poulin, Y.-K. Liu, Efficient quantum state tomography, *Nature Comm.* **2010**, 1, 150.
- [17] S. Ma, D. Goldfarb, and L. Chen, Fixed point and Bregman iterative methods for matrix rank minimization, *J. Math. Prog. A and B* **2011**, 128, 321-353.
- [18] S. Becker, J. Bobin and E.J. Candes, NESTA: A Fast and Accurate First-Order Methods for Sparse Recovery, *SIAM J. Imag. Sci.* **2011**, 4, 1-39.
- [19] S. Boyd and L. Vandenberghe, Convex Optimization, *Cambridge University Press* **2004**.
- [20] S. Mukamel, Principles of nonlinear optical spectroscopy, *Oxford University Press* **1995**.
- [21] M. Cho, Two dimensional optical spectroscopy, *CRC press, Taylor and Francis group* **2009**.
- [22] G. Engel, T. Calhoun, E. Read, T. Ahn, T. Mancal, Y. Cheng, R. Blankenship and G.R. Fleming, Evidence for wavelike energy transfer through quantum coherence in photosynthetic systems, *Nature* **2007**, 446, 782-786.
- [23] G. Panitchayangkoon, D. Hayes, K. Fransted, J. Caram, E. Harel, J. Wen, R. Blankenship, and G. Engel, Long-lived quantum coherence in photosynthetic complexes at physiological temperature, *Proceedings of the National Academy of Sciences* **2010**, 107, 12766-12770.
- [24] D. Hayes, G. Panitchayangkoon, K. A. Fransted, J. R. Caram, J. Wen, K. F. Freed, and G. S. Engel, Dynamics of electronic dephasing in the Fenna-Matthews-Olson complex, *New J. Phys.* **2010**, 12, 065042 (12 pages).
- [25] F. Caycedo-Soler, A.W. Chin, J. Almeida, S.F. Huelga, and M.B. Plenio, The nature of the low energy band of the Fenna-Matthews-Olson complex: Vibronic signatures, *J. Chem. Phys.* **2012**, 136, 155102 (13 pages).
- [26] B. Hein, C. Kreisbeck, T. Kramer, M. Rodriguez, Modelling of Oscillations in Two-Dimensional Echo-Spectra of the Fenna-Matthews-Olson Complex, *New Journal of Physics* **2012**, 14, 023018 (20 pages).
- [27] F. Caruso, S. K. Saikin, E. Solano, S. F. Huelga, A. Aspuru-Guzik and M. B. Plenio, Probing biological light-harvesting phenomena by optical cavities, *Phys. Rev. B*, **2012**, 85, 125424 (10 pages).
- [28] D. E. Tronrud, J. Wen, L. Gay and R.E. Blankenship, The structural basis for the difference in absorbance spectra for the FMO antenna protein from various green sulfur bacteria, *Photosynth. Res.* **2009**, 100, 79-87, PDB ID:3EOJ
- [29] This time scale can be improved considerably by making use of the sparsity of the matrices and algorithmic improvements [17, 18].